WILEY-VCH

X-ray Characterization of Materials

Edited by Eric Lifshin

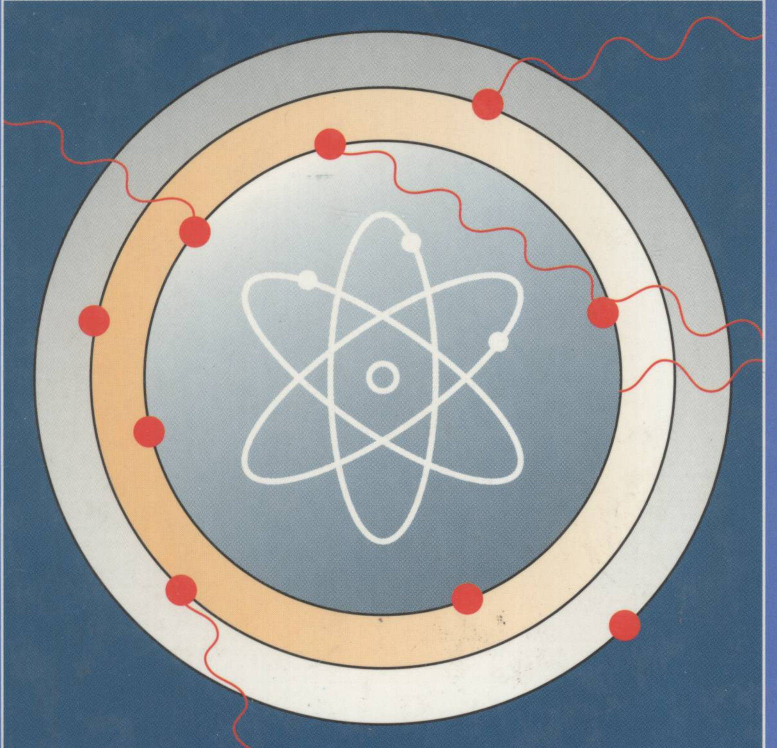

Eric Lifshin (Ed.)

X-ray Characterization of Materials

WILEY-VCH

Weinheim · New York · Chichester · Brisbane · Singapore · Toronto

materials science

Editor:
Dr. Eric Lifshin
Characterization and Environmental
Technology Laboratory
GE Corporate Research and Technology
1 Research Circle
Niskayuna, NY 12309
USA

Library of Congress Card No. applied for.

A catalogue record for this book is available from the British Library.

Deutsche Bibliothek Cataloguing-in-Publication Data:
X-ray characterization of materials / Eric Lifshin (ed.). Robert L. Snyder ... – Weinheim ; New York ; Chichester ; Brisbane ; Singapore ; Toronto : Wiley-VCH, 1999
ISBN 3-527-29657-3

Printed on acid-free and chlorine-free paper.

Composition, Printing and Bookbinding: Konrad Triltsch, Druck- und Verlagsanstalt GmbH, D-97070 Würzburg
Printed in the Federal Republic of Germany

Eric Lifshin (Editor)

X-ray Characterization of Materials

WILEY-VCH

Related titles from WILEY-VCH

S. Amelinckx, D. van Dyck, J. van Landuyt, G. van Tendeloo (Eds.)
Handbook of Microscopy
3 Vols., ISBN 3-527-29444-9

S. N. Magonov, M.-U. Whangbo
Surface Analysis with STM and AFM
ISBN 3-527-29313-2

D. Brune, R. Hellborg, H. J. Whitlow, O. Hunderi
Surface Characterization
ISBN 3-527-28843-0

Non-destructive testing
X-ray spectroscopy
Materials — Testing

Preface

It is now just over 100 years since W. C. Roentgen (1898) first discovered x-rays. His work followed by that of H. G. Mosely (1912), W. L. and W. H. Bragg (1913), and other pioneers led the way to the development of many techniques essential to the characterization of metals, ceramics, semiconductors, glasses, minerals and biological materials. X-ray diffraction, fluorescence and absorption methods provide both qualitative and quantitative information about structure and composition essential to understanding material behavior. These methods are not only used in the course of basic research, but are also critical to the development of new materials required by society as well as understanding why materials fail in service. X-ray equipment is now found in laboratories all over including facilities that support steel mills, art museums, semiconductor fabrication facilitics to cite just a few examples. Although it is not the main focus of this volume, many major advances in medicine can be linked to the findings of x-ray crystallography and various forms of radiography. Today, three-dimensional reconstruction of the human body is possible in minutes utilizing the latest in computerized tomographic clinical instrumentation.

The ability to do such remarkable diagnostic work is the result of the continuing evolution of x-ray science and technology that has drawn heavily on advances in electronics, materials science, mechanical engineering and computers. As a result, x-ray generators are more stable, tubes capable of much higher intensities, spectrometers more versatile and accurate, and detectors and associated electronics are more sensitive and capable of higher count rates. Most modern instruments also incorporate some degree of automation making control of instruments and unattended collection of data possible. A wide range of software is also readily available for phase and elemental identification, determination of strain, texture measurement, particle size distribution, single crystal structure and thin film characterization. Both commercial and "home-made" x-ray instrumentation can be found in every major industrial, academic and government laboratory.

Progress does stop, however, and over the past few decades there has been even greater interest in x-ray methods arising from the use of multi-user synchrotron facilities that provide very intense sources of radiation. Synchrotron laboratories have opened the door to the practical application of a wide variety of additional characterization techniques including x-ray absorption fine structure (EXAFS), x-ray topography and both micro-scale x-ray fluorescence and diffraction. EXAFS, for example, provides information about local atomic environments and is particularly useful in the study of catalysts even those present in concentrations below hundreds of parts per million.

This volume also covers small angle x-ray scattering (SAX), a method that can be performed with either conventional or synchrotron sources. Data obtained at low angles is indicative of grain size and shape, i.e. structure with slightly larger dimensions than atomic separation distances, which are difficult to determine in other ways. An excellent example is the determination of the radius of gyration as a function of molecular weight for polymers. Other examples include studies of phase separation in alloy systems.

The authors of the various articles present are all experts in their fields. They have done an excellent job of acquainting readers with the history, underlying principals, instrumentation, capabilities and limitations of x-ray methods as well as numerous examples of their use, and have also suggested related reading. I think all readers will find this volume a unique source of information.

Eric Lifshin
Voorheeseville, NY
5/10/99

List of Contributors

Dr. Andrea R. Gerson
University of London
Department of Chemistry
King's College
The Strand
London WC2R 2LS
UK

Dr. André Guinier
Université de Paris-Sud
Laboratoire de Physique des Solides
F-91405 Orsay Cedex
France

Dr. Peter J. Halfpenny
University of Strathclyde
Department of Pure and Applied Chemistry
295 Cathedral Street
Glasgow G1 1XL
Scotland

Dr. Ronald Jenkins
JCPDS
International Centre for Diffraction Data
1601 Park Lane
Swarthmore, PA 19801-2389
USA

Dr. Roland P. May
Institut Laue-Langevin
Avenue des Martyrs 156X
F-38042 Grenoble Cedex 9
France

Dr. Stefania Pizzini
Centre Universitaire Paris-Sud
LURE
Bâtiment 209 D
F-91405 Orsay Cedex
France

Dr. Radoljub Ristic
University of Strathclyde
Department of Pure and Applied Chemistry
295 Cathedral Street
Glasgow G1 1XL
Scotland

Dr. Kevin J. Roberts
SERC Daresbury Laboratory
Warrington WA4 4AD
UK

Dr. David B. Sheen
University of Strathclyde
Department of Pure and Applied Chemistry
295 Cathedral Street
Glasgow G1 1XL
Scotland

Professor John N. Sherwood
University of Strathclyde
Department of Pure and Applied Chemistry
295 Cathedral Street
Glasgow G1 1XL
Scotland

Prof. Robert L. Snyder
Department of Materials Science and Engineering
Ohio State University
477 Watta Hall, 2041 College Rd.
Columbus, OH 43210
USA

Dr. Claudine E. Williams
Laboratoire de Physique
CNRS URA 792
Collège de France
11, Place Marcelin Berthélot
F-75231 Paris Cedex 05
France

List of Symbols and Abbreviations

a, b, c	crystal unit cell parameters
$\boldsymbol{a}, \boldsymbol{b}, \boldsymbol{c}$	unit cell edge translation vectors
$\boldsymbol{a}^*, \boldsymbol{b}^*, \boldsymbol{c}^*$	reciprocal cell translation vectors
A	sample area
$A(\boldsymbol{q})$	scattering amplitude
b_{i}	coherent scattering length of atom i
B	bending magnet strength in Tesla (Chapter 2)
B, b	background (Chapter 3)
B, B_{ij}	Debye-Waller temperature factor and tensor components (Chapter 1)
B_{i}	spin-dependent scattering length of atom i (Chapter 4)
c	solute concentration (Chapter 4)
c	speed of light (Chapter 1)
c	velocity of light (Chapter 2)
C	concentration
d	interplanar spacing (Chapter 3)
d	lattice plane spacing (Chapter 2)
d	sample thickness (Chapter 4)
d_0	Bragg spacing
$\boldsymbol{d}_{hkl}$	interplanar spacing vector
$\boldsymbol{d}^*_{hkl}$	reciprocal cell interplanar spacings
D	particle dimension
$\mathscr{D}$	fractal dimension
e	charge on the electron
$\boldsymbol{e}, \boldsymbol{e}_0$	unit vectors along the diffracted and incident beams
e_i	energy to produce one ion pair
E	energy
E	energy of the beam (Chapter 2)
E_{p}	energy of the particle
f, f_0	atomic scattering factor
$\Delta f', \Delta f''$	anomalous dispersion scattering components
F	Fano factor
F_{hkl}	structure factor (Chapter 1)
F_i	amplitude of the backscattering factor
F_N	Smith, Synder figure of merit evaluated at line N
F_{nkl}	modulus of the structure factor (Chapter 2)
$g(r)$	radial distribution function
G	Gaussian function
h	Planck's constant
hkl	Miller indices

I	integrated diffracted intensity (Chapter 2)
I	intensity (Chapter 1)
$\boldsymbol{I}$	nuclear spin
I_0	incident intensity (Chapter 1)
I_0	incoming flux (Chapter 2)
$I_{i\alpha}$	intensity of reflection i from phase α
$I(q)$	detector counts
$I(q)$	scattered intensity
I^{rel}	relative intensity, usually on a scale of 100
I_t	transmitted flux
$I(\lambda)$	photon intensity
J	total angular momentum
k	magnitude of the photoelectron wave vector (Chapter 2)
$\boldsymbol{k}$	wave vector (magnitude: $2\pi/\lambda$) (Chapter 1)
$\boldsymbol{k}, \boldsymbol{k}_0$	scattering vectors along the diffracted and incident beams (Chapter 4)
K_0	bulk modulus
$K_{\alpha 1}, K_{\alpha 2}, K_{\beta}$	characteristic X-ray emission lines
l	angular quantum number
L	Avogadro's number (Chapter 1)
L	Lorentzian function (Chapter 1)
L	orbital angular momentum (Chapter 3)
L	sample to source distance (Chapter 2)
LLD	lower limit of detection
Lp	Lorentz and polarization corrections
m	magnetic quantum number (Chapter 3)
m	mass
m	sensitivity of X-ray fluorescence method (Chapter 3)
m_0	rest mass of the electron
m_e	mass of the electron
M	molecular mass (Chapter 4)
M	multiplicity of a plane (Chapter 1)
M_{20}	de Wolff figure of merit
n	principal quantum number
n_b, n_p	number of counts on peak (p) and background (b)
N	number of electrons (Chapter 3)
N	number of measurements (Chapter 3)
N	number of particles in the sample (Chapter 4)
N_A	Avogadro's number
N_i	co-ordination number for atoms of type i
$p(r)$	pair-distance distribution function
P	profile due to instrumental effects, the convolution of $W * G$ (Chapter 1)
P, p	peak (Chapter 3)
$P(\boldsymbol{r})$	Patterson function
$P(\lambda)$	photon flux
q	wave vector (magnitude)

$\boldsymbol{q}$	momentum transfer, $\lvert q\rvert=(4\pi/\lambda)\sin\theta$
Q	Porod's invariant
r	real-space distance
r	shell distance
r_i	radial distance from absorbing atom
R	counting rate (Chapter 3)
R	radius of a sphere (Chapter 4)
R	ratio (Chapter 3)
R	refinement factor (Chapter 2)
R	resolution (Chapter 3)
R, r	distance (Chapter 1)
$R(E)$	reflectivity coefficient
R_b, R_p	background and peak counting rates
R_g	geometrical resolution factor in X-ray topography
R_G	radius of gyration
$RIR_{\alpha,\beta}$	reference intensity ratio of phase α with respect to β
R_s	radius of the synchrotron storage ring in meters
R_t	theoretical resolution
s	spin quantum number
$\boldsymbol{s}$	neutron spin
S	profile from diffraction by the sample (Chapter 1)
S	source size (Chapter 2)
S_0	damping term for multibody effects in EXAFS analysis
S_α	Rietveld scale factor for phase α
t	sample thickness (Chapter 2)
t	time
t_b	background counting time
t_p	peak counting time
T	transmission coefficient
u	root mean square amplitude of vibration
v	partial specific volume
V	accelerating voltage (Chapter 1)
V	irradiated sample volume (Chapter 4)
V	unit cell volume (Chapter 1)
V	voltage (Chapter 3)
V_c	critical excitation potential
V_p	particle volume
W	atomic weight (Chapter 1)
W	weight fraction (Chapter 3)
$W * G$	wavelength and instrumental profiles
x	sample to film distance (Chapter 2)
x	thickness
x, y, z	atomic fractional coordinates
X	weight fraction
z	charge on the nucleus (Chapter 1)

z	number of molecules in the unit cell (Chapter 2)
Z	atomic number (Chapter 3)
Z	number of asymmetric units per unit cell (Chapter 1)
α	total absorption
α, β, γ	cell parameters (Chapter 2)
α, β, γ	interaxial angles (Chapter 1)
$\alpha^*, \beta^*, \gamma^*$	reciprocal cell interaxial angles
β	full width at half maximum of a diffraction peak
$\beta_\varepsilon, \beta_\tau$	peak broadening due to strain and size
$\gamma(r)$	correlation function
Γ	shear gradient
δ	deviation parameter for an incommensurate phase
ε	detector efficiciency (Chapter 4)
ε	residual lattice stress (Chapter 1)
θ	Bragg diffraction angle
2θ	scattering angle
θ_m	diffraction angle of monochromator
Θ	vertical divergence of the beam
Θ_B	Bragg angle
λ	wavelength
λ_c	critical wavelength
λ_d	damping factor used in EXAFS analysis to allow for inelastic scattering effects
λ_{SWL}	short wavelength limit from an X-ray tube
μ	linear absorption coefficient
μ_0	absorption of an atom in the absence of neighbors (Chapter 1)
μ_0	background absorption (Chapter 2)
μ/ϱ	mass absorption coefficient
ν	frequency
$\bar{\nu}$	wave number
ϱ	density
$\varrho(r), \varrho(xyz)$	electron density at location r or xyz
σ	counting error
σ	shielding constant
σ	standard deviation
$d\sigma(q)/d\Omega$	scattering cross section per particle and unit solid angle
$d\Sigma(q)/d\Omega$	macroscopic differential cross section
σ_i	Debye-Waller type factor used in EXAFS analysis (Chapter 2)
σ_i	displacement between absorbing atoms (Chapter 1)
σ_{net}	net counting error
$\sigma_{(N)}$	random error
τ	crystallite size
ϕ	fixed incident glancing angle (Chapter 2)
ϕ	phase angle (Chapter 1)
ϕ	volume fraction occupied by matter (Chapter 4)

ϕ_c	critical angle for total external reflection
Φ_i	phase shift function used in EXAFS analysis
ψ	binding energy (Chapter 3)
ψ	wave function (Chapter 1)
ω	fluorescent yield
$\Delta\Omega$	solid angle subtended by a detection element
χ	EXAFS interference function
$\chi(k)$	EXAFS function

ADP	ammonium dihydrogen phosphate
ASAXS	anomalous small-angle X-ray scattering
b.c.c.	body-centred cubic
BNL/NSLS	Brookhaven National Laboratory National Synchrotron Light Source
CD-ROM	compact disk read only memory
CVD	chemical vapor deposition
DCD	double-crystal diffractometer
EDD	electron diffraction database
EDS	energy dispersive spectroscopy
EDXRD	energy dispersive X-ray diffraction
EISI	elemental and interplanar spacings index
EXAFS	extended X-ray absorption fine structure
f.c.c.	face-centred cubic
FET	field effect transistor
FOM	figure of merit
FWHM	full width at half maximum
ICDD	international centre for diffraction data
IFT	indirect Fourier transformation
ITO	indium/tin oxide
IUPAC	international union of pure and applied chemistry
KZC	K_2ZnCl_4
LSM	layered synthetic micro-structure
MBA-NB	(–)-2-(α-methylbenzylamino)-5-nitropyridine
MBE	molecular beam epitaxy
MCA	multichannel analyzer
ML	monolayers
NF	nickel formate dihydrate
PC	desktop computer
PDF	powder diffraction file
PHA	pulse height analyzer
PIXE	proton excited X-ray fluorescence
PSD	position sensitive detector
PTS	2,4-hexadiynediol-bis-(*p*-toluene sulfonate)
QEXAFS	quick-scanning EXAFS
RDF	radial distribution function
ReflEXAFS	reflectivity EXAFS

SANS	small-angle neutron scattering
SAS	small-angle scattering
SAXS	small-angle X-ray scattering
SR	synchrotron radiation
SSXRF	synchrotron source X-ray fluorescence
TAP	thallium acid phtalate
TEM	transmission electron microscopy
TOF	time of flight
TRXRF	total reflection X-ray fluorescence
WDS	wavelength dispersive spectroscopy
XAS	X-ray absorption spectroscopy
XANES	X-ray absorption near-edge structure
XRD	X-ray diffraction
XRF	X-ray fluorescence
XSW	X-ray standing waves
ZBH	zero background holder

Contents

1 X-Ray Diffraction

Robert L. Snyder

Institute for Ceramic Superconductivity, New York State College of Ceramics, Alfred University, Alfred, NY, U.S.A.